ENVIRONMENTAL STUDIES

Past and future drought in Mongolia

Amy E. Hessl,[1]* Kevin J. Anchukaitis,[2] Casey Jelsema,[3] Benjamin Cook,[4,5] Oyunsanaa Byambasuren,[6] Caroline Leland,[4] Baatarbileg Nachin,[6] Neil Pederson,[7] Hanqin Tian,[8] Laia Andreu Hayles[4]

The severity of recent droughts in semiarid regions is increasingly attributed to anthropogenic climate change, but it is unclear whether these moisture anomalies exceed those of the past and how past variability compares to future projections. On the Mongolian Plateau, a recent decade-long drought that exceeded the variability in the instrumental record was associated with economic, social, and environmental change. We evaluate this drought using an annual reconstruction of the Palmer Drought Severity Index (PDSI) spanning the last 2060 years in concert with simulations of past and future drought through the year 2100 CE. We show that although the most recent drought and pluvial were highly unusual in the last 2000 years, exceeding the 900-year return interval in both cases, these events were not unprecedented in the 2060-year reconstruction, and events of similar duration and severity occur in paleoclimate, historical, and future climate simulations. The Community Earth System Model (CESM) ensemble suggests a drying trend until at least the middle of the 21st century, when this trend reverses as a consequence of elevated precipitation. Although the potential direct effects of elevated CO_2 on plant water use efficiency exacerbate uncertainties about future hydroclimate trends, these results suggest that future drought projections for Mongolia are unlikely to exceed those of the last two millennia, despite projected warming.

INTRODUCTION

Recent droughts in semiarid regions had few, if any, analogs in the historical record, and although exceptionally rare (*1*–*3*), they may have occurred in the absence of greenhouse forcing. However, as global temperatures rise, potential evapotranspiration (PET), a measure of moisture demand, is expected to become an increasingly important factor in the severity of drought (*4*, *5*), posing serious threats to ecosystems (*6*) and societies (*7*, *8*). Although climate model projections indicate that within the next few decades "hot droughts" will become increasingly frequent and severe in semiarid regions (*9*–*11*), precipitation forecasts remain less certain, resulting in widely varying projections of moisture under future climate change (*12*).

Northern Asia experienced rapid warming (0.3° to 0.7°C per decade) between 1950 and 2010 (*13*). In the next century, precipitation is expected to increase over arid Inner Asia, though these projections have only medium confidence (*14*), and the combined effects of elevated temperature and variable precipitation on drought are still unknown. In Mongolia, mean annual temperatures rose approximately 0.4°C between 1951 and 1990 (*15*), with continued warming since the 1990s (Fig. 1B). Recent drought in Mongolia has been associated with major social and environmental change, including a migration of several hundred thousand herders to the capital city, loss of lakes, and declines in grassland productivity (*16*–*18*). Although both scholarly and popular sources have attributed these droughts to anthropogenic climate change, the instrumental record of moisture is spare and the satellite record short, making it difficult to assess whether 21st century drying is without precedent. Multicentennial reconstructions of past temperature for both Mongolia and Asia indicate that growing season temperatures are now ~1.5°C higher than those in the previous several centuries (*19*). Coincident with these increases in temperature, extensive regions of the Mongolian Plateau experienced a prolonged and severe drought in the early 2000s (Fig. 1A) (*17*, *20*), attributed to rising land and ocean temperatures (*21*, *22*). Precipitation during this drought was anomalously low, and analysis of the temperature and precipitation contributions to the PDSI indicates that a third of the drought's overall intensity could have been caused by elevated temperature (fig. S1), making this event unusual during the instrumental period. Few long records exist to test whether this event is unusual over longer time scales—an important consideration given the extreme moisture variability of the Mongolian Plateau. A previous drought reconstruction for Mongolia, derived from tree ring data from a single site, suggested that the recent drought was unusual over the last millennium (*23*). Here, we use a 2060-year tree ring reconstruction of summer drought from two sites in central Mongolia to evaluate whether recent drying was unprecedented in its joint duration and severity over the Common era. We then use an ensemble of general circulation model simulations to place the recent event in the context of past natural variability and expected changes in the future as a consequence of anthropogenic climate change.

RESULTS

We developed a 2060-year, annually dated reconstruction of drought (using tree rings from two sites in central Mongolia) that accounts for 72% of the variability in self-calibrating PDSI, hereafter PDSI (*24*) over Mongolia and portions of northeastern China during the calibration period (1959–2011) (Fig. 1, C and D). Our reconstruction indicates that the late 20th and early 21st centuries witnessed both one of the driest—as well as one of the wettest—periods in the last 2060 years (Fig. 2). A 5-year pluvial beginning in 1990 with a cumulative reconstructed PDSI of 7.7 exceeds the estimated 1000-year return time based on joint distributions of pluvial duration and magnitude (Fig. 2A). This extremely wet period was followed by the 21st-century drought with a duration of 12 years, a cumulative PDSI of −22.3, and an estimated return time of more than 900 years (Fig. 2B). Longer droughts [for example, a 16-year drought beginning in 1175 with a cumulative reconstructed June-to-September

[1]Department of Geology and Geography, West Virginia University, 98 Beechurst Avenue, Morgantown, WV 26501, USA. [2]School of Geography and Development and Laboratory of Tree-Ring Research, University of Arizona, AZ 85721, USA. [3]Department of Statistics, West Virginia University, Morgantown, WV 26506, USA. [4]Lamont-Doherty Earth Observatory, Columbia University, Palisades, NY 10964, USA. [5]NASA Goddard Institute for Space Studies, New York, NY 10025, USA. [6]Department of Forestry, National University of Mongolia, Ulaanbaatar, Mongolia. [7]Harvard Forest, Harvard University, Petersham, MA 01366, USA. [8]School of Forestry and Wildlife Sciences, Auburn University, Auburn, AL 36849, USA.
*Corresponding author. Email: amy.hessl@mail.wvu.edu

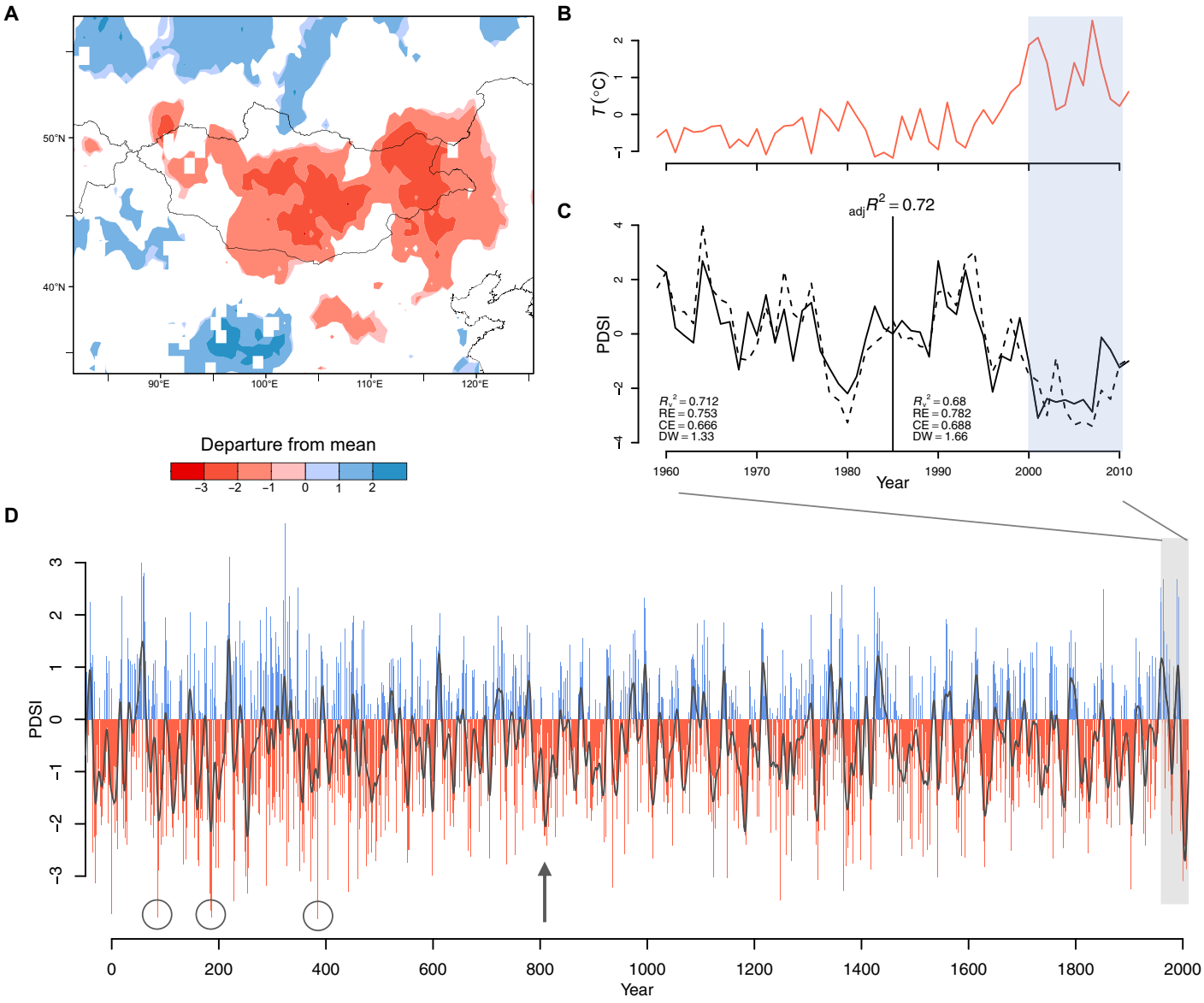

Fig. 1. The 21st-century drought. (**A**) Self-calibrating Palmer Drought Severity Index (PDSI) anomalies across Asia (2000–2010 and 1959–2011 reference periods) (*24*). (**B**) Observed temperature anomalies (NASA Goddard Institute for Space Studies) (*42*) over Mongolia (1959–2011 reference period). (**C**) Reconstructed (black) and observed (dashed) PDSI with 2000–2010 drought highlighted (blue bar), and split calibration/verification period (vertical line) statistics including verification R^2 (R_v^2), reduction of error (RE), coefficient of efficiency (CE), Durbin-Watson statistic (DW), and overall $_{adj}R^2$ for entire calibration period. (**D**) Reconstructed PDSI (49 BCE–2011 CE). Shown are blue (PDSI > 0) and red (PDSI < 0) bars with a 15-year spline (black line) centered on the mean of the calibration period (1959–2011). More severe single-year droughts (86, 186, and 385 CE) are marked with open circles, and the severe drought beginning in 804 CE is indicated with an arrow.

(JJAS) PDSI of −21.5] and a single more severe drought (a 19-year drought beginning in 804 with a cumulative reconstructed JJAS PDSI of −24.9) occurred during the Medieval Climate Anomaly, even though independent tree ring reconstructed temperatures were cooler during this period relative to recent decades (*25*). Individual years (for example, 86, 186, and 385 CE) exceed the lowest values reconstructed for the 21st-century drought (2001 CE is ranked as the 17th driest out of 2060 years), although these extreme single-year events are based on data from a single site (Fig. 1D and figs. S2 and S3).

To better understand the relative role of internal climate system variability and radiative forcing in causing hydroclimate anomalies in the past and future, we use our long tree ring reconstructions of past PDSI in concert with ensemble simulations from coupled atmosphere-ocean climate models. We take advantage of the Community Earth System Model (CESM) Last Millennium Ensemble (LME) (*26*) and its extension to the year 2100 using the Representative Concentration Pathway 8.5 (RCP8.5 emissions scenario, which is designed to yield an approximate top-of-atmosphere radiative imbalance of +8.5 W m^{-2} by 2100), to investigate whether CESM can reproduce the statistics of reconstructed drought variability over the last millennium. Then we determine what the model ensemble predicts for future drought severity and duration for Mongolia through the end of this century. The paleoclimate model ensemble spans the distribution of variability seen over the full 2060 years of our tree ring proxy reconstruction, providing confidence that

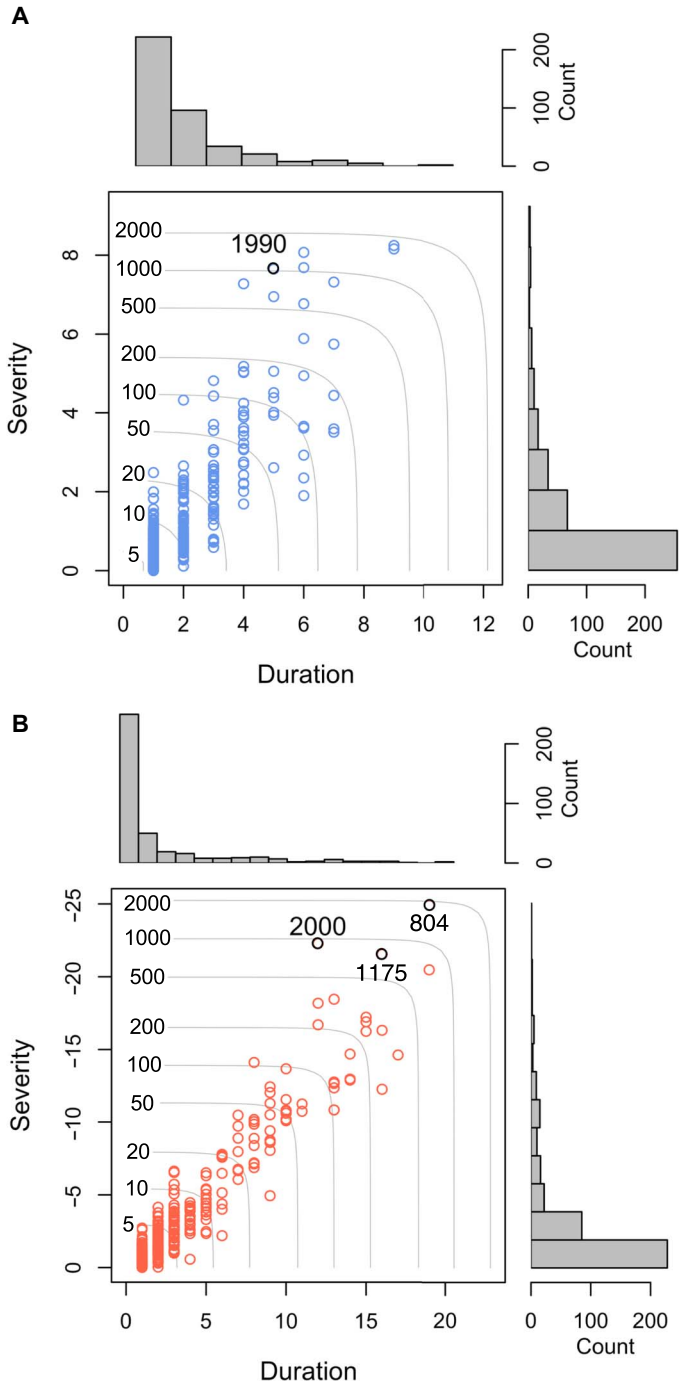

Fig. 2. Runs analysis and estimated return time of pluvials and droughts. (**A**) Cumulative severity and duration of pluvials (blue circles) and (**B**) droughts (red circles) based on reconstructed continuous runs of high self-calibrating PDSI > 0 and PDSI < 0, respectively, with counts for each variable in the margins (gray bars). Contours of return time (gray) were derived from copula functions for the joint probability of severity and duration of pluvial and drought events. The pluvial beginning in 1990 and the droughts beginning in 804, 1175, and 2000 are denoted with black circles.

these simulations can produce the range of hydroclimate conditions captured by the tree rings over the last millennium (Fig. 3, A and B). However, the individual ensemble members from CESM all have PDSI variance that is larger than the reconstruction, which merits caution in the interpretation of the absolute magnitude of simulated past and future drought. Consistent with previous findings in other regions (*27*, *28*), past droughts in the simulations (as well as the reconstruction) appear not to be forced—that is, they arise as a feature of internal climate system variability. As a result, the model ensemble members are uncorrelated at both interannual and decadal scales throughout the last millennium.

We find that climate and radiative controls on future drought variability are both timescale-dependent and uncertain. Interannual- to decadal-scale droughts continue to occur in the future RCP8.5 scenarios through 2100. The distribution of interannual drought severity does indicate an increased number of more severe droughts compared with the last millennium simulations (Fig. 3C). However, in the simulated future, multiyear joint drought duration and cumulative severity fall entirely within the range of the historical and last millennium simulations, and longer and more severe unforced droughts occur in the model simulations before the 21st century (Fig. 3D).

We find that the underlying multidecadal- to centennial-scale trends are set by the timing and magnitude of long-term forced changes in both temperature and precipitation. In the CESM LME +RCP8.5 simulations, greenhouse gas forcing through the end of the 21st century results in an increase in summer precipitation in Mongolia, apparently as the direct thermodynamic response to increased air temperature through an increase in precipitable water. Likewise, in all the CESM LME +RCP8.5 ensemble members, summer surface air temperature in Mongolia increases through 2100. This increase in temperature and the associated increase in evaporative demand initially drive the system toward an overall drier state (more negative PDSI) in all RCP8.5 ensemble members (Fig. 4A). By mid-century, however, the simulated increase in precipitation begins to compensate for the trends in evaporative demand, and all ensemble members trend back toward the long-term mean hydroclimate state (Fig. 4A). The forced trends in precipitation and temperature cause the CESM ensemble members to be more similar through the 21st century than for the last millennium and historical periods.

Across the full Coupled Model Intercomparison Project Phase 5 (CMIP5) RCP8.5 ensemble, some similar patterns emerge for central Mongolia (Fig. 4A) (*4*). The span of future drought conditions includes a range of both positive and negative trends through 2100, with each individual model response dependent on the timing and magnitude of that model's overall upward trends in both PET and precipitation (Fig. 4, B and C). The CMIP5 multimodel mean has a smaller transient signal, with a late 21st century drying trend partially mediated by the influence of increased precipitation by the end of the 21st century (Fig. 4, A and C). However, because of the different combinations of precipitation and temperature trends in the CMIP5 models, the ensemble overall spans a range of possible trends of different signs, and this uncertainty dominates the multimodel future projected trends.

Together, the model simulations and paleoclimate data suggest that the recent droughts were unusual but were not unprecedented over the last two millennia. Model simulations also reveal considerable uncertainty about future long-term drought and changes in the mean hydroclimate state in Mongolia. Further, accounting for the influence of higher atmospheric CO_2 on plant transpiration and water use efficiency, reduced evapotranspiration from the land surface leads to increased soil moisture when calculated directly within the CESM's land surface model (Fig. 4D). However, the physiological response of vegetation transpiration to rising CO_2 can vary considerably across different models and in manipulation experiments, further exacerbating uncertainty (*12*, *29*–*31*). An additional uncertainty is the impact of future aerosol

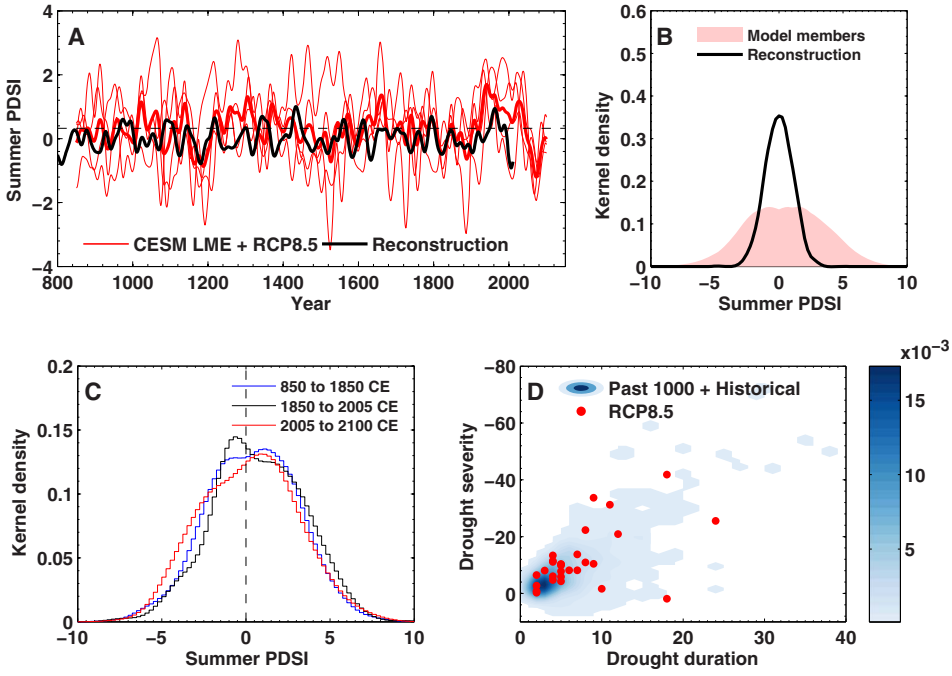

Fig. 3. Past, present, and future drought in paleoclimate reconstructions and Community Earth System Model (CESM) model simulations. (**A**) CESM Last Millennium Ensemble (LME)–simulated (red) and tree ring reconstructed (black) Penman-Monteith PDSI for Central Mongolia. Thin red lines are individual ensemble members from CESM LME that have an extension to 2100 using the Representative Concentration Pathway 8.5 (RCP8.5) scenario. The heavy red line is the ensemble mean. All time series have been smoothed with a 30-year Gaussian filter. (**B**) Kernel probability density estimate for the individual ensemble member simulated and the tree ring reconstructed annual PDSI values used in (A). (**C**) Kernel probability density estimates for the CESM LME model simulated PDSI for three periods: the last millennium (850–1850), historical (1850–2005), and future RCP8.5 (2005–2100), showing an increased occurrence of the most severe annual drought index values under the future greenhouse gas forcing scenario. (**D**) Bivariate kernel density of joint drought duration and severity from the CESM LME ensemble for multiyear (2 years or more) events. Blue shading shows the joint distribution for the model last millennium and historical periods, whereas red circles indicate multiyear drought events under the future RCP8.5 forcing.

reduction, which model simulations suggest could exacerbate aridity over some regions of Mongolia because of an increase in surface temperature and PET (*32*).

DISCUSSION

Extremes in moisture such as the 1990s pluvial and the 2000s drought are extraordinarily rare over the Common era in Mongolia but not without precedent in the last 2060 years. On the basis of our reconstructions, both of these events exceed the 900-year return interval, even when the amplitude of the reconstruction is scaled to that of the instrumental target (fig. S7). There is a rather large uncertainty in projections of the future drought trajectory for Mongolia, which is dependent on the relative contributions of increasing evaporative demand, anticipated increases in precipitation, and the physiological response of vegetation to rising CO_2. Previous studies have observed that the balance of temperature and precipitation effects on future drought can result in drying irrespective of the uncertainties in future precipitation trends (*33*) but that changes in drought risk in response to rising temperature vary regionally and may be highly uncertain (*34*). A novel observation here is that the relative importance of temperature and precipitation on drought is time-dependent in the CESM ensemble, with initial drying trends in Mongolia eventually reversed by increasing precipitation, although this feature is present to a much lesser degree in the full CMIP5 multimodel mean. If a time-dependent pattern of hydroclimate change occurs for continental semiarid regions because of the timing of precipitation increases, then this could have implications for the detection and attribution of anthropogenic forced changes in hydroclimate as well as for water management.

In regions where nearly all the wet season precipitation comes from continental source areas, there are likely strong feedbacks between the land, land cover, and atmosphere that may create persistence in hydroclimate conditions. As temperatures continue to warm, the role of moisture delivery to Inner Asia and accurate projections of future precipitation become increasingly critical, as does an improved understanding of how ecological feedbacks from rising CO_2 may ameliorate or exacerbate climatic trends. Although the threat of multiyear droughts such as those observed in the paleoclimate record persists through the coming decades, model projections indicate that these are unlikely to exceed those experienced over the last two millennia. Nevertheless, planning and adaptation are complicated by wide uncertainties in climate forecasts. Resolving these uncertainties should remain a focus of climate modeling given the potential consequences for both societies and ecosystems.

MATERIALS AND METHODS

We collected Siberian pine increment cores and cross sections from two Holocene basaltic lavas, Khorgo (KLP) and Uurgat (ULP), in north central Mongolia. We collected samples from living trees growing in thin soils and from dead trees perched on basalt. Trees growing on the lavas today are widely spaced and stunted and appear severely moisture-limited. Annual ring width variability is likely indicative of past moisture availability. We measured total ring width to ±0.001 mm and cross-dated samples using standard dendrochronological procedures.

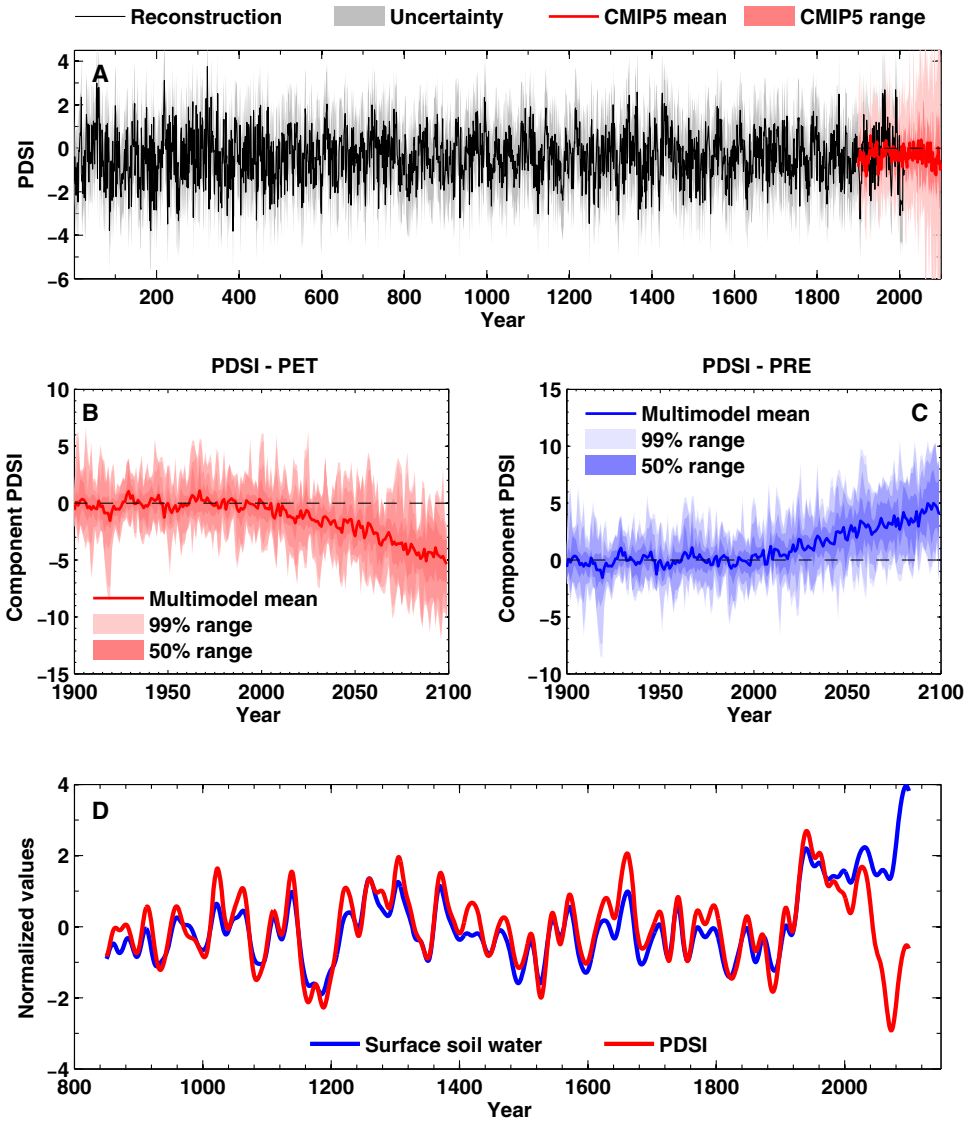

Fig. 4. Uncertainties in future moisture projections. (**A**) Reconstructed (black) and Coupled Model Intercomparison Project Phase 5 (CMIP5)–simulated (red) PDSI. Gray shading around the reconstruction indicates uncertainty as the root mean square error of the reconstruction. Pink shading around the CMIP5 ensemble mean (red line) shows the two-tailed 99% range estimated from all individual ensemble members. (**B**) CMIP5-simulated PDSI–potential evapotranspiration (PET) calculated using detrended precipitation values over 2000 to 2099. (**C**) CMIP5-simulated PDSI precipitation (PRE) using detrended temperature, net radiation, and vapor pressure over 2000 to 2099. (**D**) CESM LME ensemble mean calculated PDSI (red line) compared to online simulated CESM land surface model near-surface soil moisture (blue). Both time series have been smoothed using a 30-year Gaussian filter.

Detrending tree ring series can exaggerate trends at the end of a measurement series, a particular concern here given the timing of the 1990s pluvial and 2000s drought. We experimented with several detrending procedures, including conservative techniques, signal-free standardization, and no detrending (raw series), to evaluate the effect of detrending on the final chronologies. The severity of the 21st-century drought, as represented by conservative techniques, was most similar to that of chronologies built using the raw (not detrended) series as well as to the instrumental record. To maintain low-frequency information but reduce age-related trends in growth unrelated to climate, we used conservative techniques in the program ARSTAN to detrend and standardize the raw ring width series (*35*). We selected detrending techniques using a hierarchical framework, beginning with any of the following: a negative exponential curve or straight line with a slope of ≤0 (typically samples containing or close to pith), a straight line with a slope of 0 (typically nonstrip bark samples without early growth), or a straight line with a slope of >0 (typically strip bark samples). Three samples from KLP and two from ULP with unusual growth trends (step changes in growth) were standardized using the Friedman Super Smoother ($\alpha = 9$). We combined the individual series of tree ring indices from each site into two site chronologies using a biweight robust mean (*36*). The chronologies extend back to 668 BCE (KLP) and 416 BCE (ULP) (figs. S2 and S3), but were truncated to the period where the average expressed population signal, a metric that quantifies how well a chronology based on a finite number of trees represents a hypothetical perfect or "true" chronology, is >0.85 and sample depth was >9 (49 BCE–2011 CE for KLP and 488–2011 CE for ULP). The average correlation between tree ring series

(rbar) during the common period is 0.65 (KLP) and 0.53 (ULP), indicating that tree growth at both sites is associated with a common climate signal.

Mongolia's climate stations are sparse and have missing data, particularly since 1980. Rather than using the instrumental data directly, we used the gridded self-calibrating PDSI derived from the Climate Research Unit at University of East Anglia (CRU) 3.20 precipitation and PET fields (*24*). PDSI, as calculated here, uses the physically based Penman-Monteith equation for PET rather than the Thornthwaite function typically used in PDSI. The Penman-Monteith equation incorporates daily temperature, radiation, wind speed, and humidity, whereas the Thornthwaite uses only temperature and day length.

We reconstructed average JJAS PDSI (target) using a linear regression model relating JJAS PDSI from a grid box (46° to 49°N, 99° to 109°E) to the mean of our detrended KLP and ULP ring width chronologies over the 1959–2011 period (Fig. 1C). The grid box was defined on the basis of spatial field correlations with PDSI over Mongolia (fig S4, A and C). We then validated our model and estimated prediction error (fig. S5) using a split-period cross-validation approach by partitioning our time series into two periods (1959–1986 and 1987–2011). To evaluate the model fit, we used calibration and validation R^2, reduction of error, and coefficient of efficiency. For the period before 488 CE, we appended a reconstruction based only on a linear model for the KLP record.

To examine the joint probability of event duration and severity, we calculated the duration and cumulative sum of PDSI during "runs" (multiple years when conditions extend below or above PDSI = 0). Analyses of these runs are sensitive to the threshold value such that the duration, severity, and timing of events change with adjustments in the definition of what constitutes a drought or a pluvial. Nevertheless, runs above or below a constant threshold can be used to characterize the duration and severity of reconstructed extremes relative to the entire reconstructed record. We estimated the joint probability of reconstructed drought and pluvial duration and severity to derive estimates of return time. Duration and severity each have different distributions and are typically correlated, necessitating a joint probability approach. One could specify joint distributions directly; for example, González and Valdés (*37*) specified a marginal geometric distribution for the duration, and conditionally upon the duration, a γ distribution for the severity. Alternatively, Shiau (*38*) used bivariate copulas to model the dependence between duration and severity. Copulas are multivariate distributions that link two or more univariate marginal distributions. An advantage of using copulas to model correlated phenomena such as the duration and severity of a drought is that one is able to specify marginal distributions on each random variable. The dependence is separately modeled through the copula function, bypassing the need to specify a more complex joint distribution. For these reasons, we used the copula approach to jointly model the duration and severity. Estimation of copula parameters was done via the copula package (*39*) in the R programming language. Similar to Shiau (*38*), we fitted multiple copula models and selected the model that maximizes the log likelihood. A challenge in determining the marginal distributions was the presence of many extreme values in the data. We explored a number of candidates for the marginal distributions and determined that exponential and γ distributions were the best fits to model duration and severity, respectively (fig. S6). Although reconstructions using linear regression reduce the SD of the reconstruction (*40*), in sensitivity analysis, we found that restoring the variance to match the calibration period generates more severe events but does not change their duration or their return time relative to other events in the record (fig. S7). To avoid inflating the error variance, we opted to use the original reconstruction in the runs and copula analysis, though we provide results with the variance adjusted to the instrumental PDSI in the Supplementary Materials (fig. S7).

We used the National Center for Atmospheric Research's CESM LME with extension to 2100 using the RCP8.5 scenario (*26*). We used model simulation monthly precipitation, net radiation, temperature, wind, and vapor pressure to calculate the JJAS PDSI for central Mongolia (46° to 49°N, 99° to 109°E) using the Penman-Monteith method to calculate PET (*4*, *5*). We used the four CESM LME ensemble members spanning the period 850–2100 CE. We also evaluated the near-surface soil moisture content from the CESM LME members. We further supplemented our analysis using three different calculations of the PDSI for central Mongolia from the full CMIP5 historical and future RCP8.5 ensemble (*4*): PDSI-ALL, including modeled changes in both PET and precipitation; PDSI-PET, using detrended precipitation values from 2000 to 2099 to isolate the impact of changes in evaporative demand; and PDSI-PRE, using detrended temperature, vapor pressure, and net radiation variables to isolate the influence of changes in precipitation. We estimated the probability density of reconstructed and simulated data using the nonparametric Gaussian kernel smoothing function (*41*).

SUPPLEMENTARY MATERIALS

Supplementary material for this article is available at http://advances.sciencemag.org/cgi/content/full/4/3/e1701832/DC1

fig. S1. PDSI for central Mongolia (99° to 107°E, 46° to 49°N) from observational and reanalysis data.
fig. S2. KLP tree ring chronology used to develop the reconstruction is robust back to 49 BCE.
fig. S3. ULP tree ring chronology used to develop the reconstruction is robust back to 488 CE.
fig. S4. The two tree ring chronologies are both high-fidelity recorders of past drought for Mongolia.
fig. S5. Upper and lower RMSE of the PDSI reconstruction.
fig. S6. Quantile-quantile fits of duration and severity for pluvials and droughts.
fig. S7. Pluvial and drought analysis using adjusted SD reconstruction.
References (*43*–*45*)

REFERENCES AND NOTES

1. B. I. Cook, K. J. Anchukaitis, R. Touchan, D. M. Meko, E. R. Cook, Spatiotemporal drought variability in the Mediterranean over the last 900 years. *J. Geophys. Res. Atmos.* **121**, 2060–2074 (2016).
2. S. Belmecheri, F. Babst, E. R. Wahl, D. W. Stahle, V. Trouet, Multi-century evaluation of Sierra Nevada snowpack. *Nat. Clim. Change* **6**, 2–3 (2016).
3. D. Griffin, K. J. Anchukaitis, How unusual is the 2012–2014 California drought? *Geophys. Res. Lett.* **41**, 9017–9023 (2014).
4. B. I. Cook, J. E. Smerdon, R. Seager, S. Coats, Global warming and 21st century drying. *Clim. Dyn.* **43**, 2607–2627 (2014).
5. K. B. Karnauskas, J. P. Donnelly, K. J. Anchukaitis, Future freshwater stress for island populations. *Nat. Clim. Chang.* **6**, 720–725 (2016).
6. A. P. Williams, C. D. Allen, A. K. Macalady, D. Griffin, C. A. Woodhouse, D. M. Meko, T. W. Swetnam, S. A. Rauscher, R. Seager, H. D. Grissino-Mayer, J. S. Dean, E. R. Cook, C. Gangodagamage, M. Cai, N. G. McDowell, Temperature as a potent driver of regional forest drought stress and tree mortality. *Nat. Clim. Chang.* **3**, 292–297 (2013).
7. A. I. J. M. van Dijk, H. E. Beck, R. S. Crosbie, R. A. M. de Jeu, Y. Y. Liu, G. M. Podger, B. Timbal, N. R. Viney, The Millennium Drought in southeast Australia (2001–2009): Natural and human causes and implications for water resources, ecosystems, economy, and society. *Water Resour. Res.* **49**, 1040–1057 (2013).
8. A. F. Van Loon, T. Gleeson, J. Clark, A. I. J. M. Van Dijk, K. Stahl, J. Hannaford, G. Di Baldassarre, A. J. Teuling, L. M. Tallaksen, R. Uijlenhoet, D. M. Hannah, J. Sheffield, M. Svoboda, B. Verbeiren, T. Wagener, S. Rangecroft, N. Wanders, H. A. J. Van Lanen, Drought in the Anthropocene. *Nat. Geosci.* **9**, 89–91 (2016).
9. B. I. Cook, T. R. Ault, J. E. Smerdon, Unprecedented 21st century drought risk in the American Southwest and Central Plains. *Sci. Adv.* **1**, e1400082 (2015).
10. J. Overpeck, B. Udall, Dry times ahead. *Science* **328**, 1642–1643 (2010).
11. T. Zhao, A. Dai, The magnitude and causes of global drought changes in the twenty-first century under a low–moderate emissions scenario. *J. Clim.* **28**, 4490–4512 (2015).

12. P. C. D. Milly, K. A. Dunne, Potential evapotranspiration and continental drying. *Nat. Clim. Chang.* **6**, 946–949 (2016).
13. GISTEMP Team, *GISS Surface Temperature Analysis (GISTEMP)* (NASA Goddard Institute for Space Studies, 2017).
14. IPCC, *Climate Change 2013: The Physical Science Basis* (Cambridge Univ. Press, 2013).
15. A. Yatagai, T. Yasunari, Interannual variations of summer precipitation in the arid/semi-arid regions in China and Mongolia : Their regionality and relation to the Asian summer monsoon. *J. Meteorol. Soc. Jpn. Ser. II* **73**, 909–923 (1995).
16. G. Bao, Z. Qin, Y. Bao, Y. Zhou, W. Li, A. Sanjjav, NDVI-based long-term vegetation dynamics and its response to climatic change in the Mongolian Plateau. *Remote Sens.* **6**, 8337–8358 (2014).
17. S. Tao, J. Fang, X. Zhao, S. Zhao, H. Shen, H. Hu, Z. Tang, Z. Wang, Q. Guo, Rapid loss of lakes on the Mongolian Plateau. *Proc. Natl. Acad. Sci. U.S.A.* **112**, 2281–2286 (2015).
18. M. Andrei, Riders under storms: Contributions of nomadic herders' observations to analysing climate change in Mongolia. *Glob. Environ. Change* **20**, 162–176 (2010).
19. N. K. Davi, R. D'Arrigo, G. C. Jacoby, E. R. Cook, K. J. Anchukaitis, B. Nachin, M. P. Rao, C. Leland, A long-term context (931–2005 C.E.) for rapid warming over Central Asia. *Quat. Sci. Rev.* **121**, 89–97 (2015).
20. J. Li, E. R. Cook, R. D'Arrigo, F. Chen, X. Gou, Moisture variability across China and Mongolia: 1951–2005. *Clim. Dyn.* **32**, 1173–1186 (2008).
21. K. Wei, L. Wang, Reexamination of the aridity conditions in arid Northwestern China for the last decade. *J. Climate* **26**, 9594–9602 (2013).
22. J. Piao, W. Chen, K. Wei, Y. Liu, H.-F. Graf, J.-B. Ahn, A. Pogoreltsev, An abrupt rainfall decrease over the Asian inland plateau region around 1999 and the possible underlying mechanism. *Adv. Atmos. Sci.* **34**, 456–468 (2017).
23. N. Pederson, A. E. Hessl, N. Baatarbileg, K. J. Anchukaitis, N. D. Cosmo, Pluvials, droughts, the Mongol Empire, and modern Mongolia. *Proc. Natl. Acad. Sci.* **111**, 4375–4379 (2014).
24. G. van der Schrier, J. Barichivich, K. R. Briffa, P. D. Jones, A scPDSI-based global dataset of dry and wet spells for 1901–2009. *J. Geophys. Res. Atmos.* **118**, 4025–4048 (2013).
25. E. R. Cook, P. J. Krusic, K. J. Anchukaitis, B. M. Buckley, T. Nakatsuka, M. Sano, PAGES Asiak Members, Tree-ring reconstructed summer temperature anomalies for temperate East Asia since 800 C.E. *Clim. Dyn.* **41**, 2957–2972 (2013).
26. B. L. Otto-Bliesner, E. C. Brady, J. Fasullo, Climate variability and change since 850 CE: An ensemble approach with the Community Earth System Model. *Bull. Am. Meteorol. Soc.* **97**, 735–754 (2015).
27. S. Coats, J. E. Smerdon, K. B. Karnauskas, R. Seager, The improbable but unexceptional occurrence of megadrought clustering in the American West during the Medieval Climate Anomaly. *Environ. Res. Lett.* **11**, 074025 (2016).
28. S. Coats, J. E. Smerdon, B. I. Cook, R. Seager, Are simulated megadroughts in the North American Southwest forced? *J. Climate* **28**, 124–142 (2014).
29. E. A. Ainsworth, A. Rogers, The response of photosynthesis and stomatal conductance to rising [CO_2]: Mechanisms and environmental interactions. *Plant Cell Environ.* **30**, 258–270 (2007).
30. F. A. Dijkstra, D. Blumenthal, J. A. Morgan, D. R. LeCain, R. F. Follett, Elevated CO_2 effects on semi-arid grassland plants in relation to water availability and competition. *Funct. Ecol.* **24**, 1152–1161 (2010).
31. A. L. S. Swann, F. M. Hoffman, C. D. Koven, J. T. Randerson, Plant responses to increasing CO_2 reduce estimates of climate impacts on drought severity. *Proc. Natl. Acad. Sci. U.S.A.* **113**, 10019–10024 (2016).
32. L. Lin, Z. Wang, Y. Xu, Q. Fu, Sensitivity of precipitation extremes to radiative forcing of greenhouse gases and aerosols. *Geophys. Res. Lett.* **43**, 9860–9868 (2016).
33. T. R. Ault, J. S. Mankin, B. I. Cook, J. E. Smerdon, Relative impacts of mitigation, temperature, and precipitation on 21st-century megadrought risk in the American Southwest. *Sci. Adv.* **2**, e1600873 (2016).
34. F. Lehner, S. Coats, T. F. Stocker, A. G. Pendergrass, B. M. Sanderson, C. Raible, J. E. Smerdon, Projected drought risk in 1.5°C and 2°C warmer climates. *Geophys. Res. Lett.* **44**, 7419–7428 (2017).
35. E. R. Cook, thesis, University of Arizona (1985).
36. E. R. Cook, K. Peters, Calculating unbiased tree-ring indices for the study of climatic and environmental change. *Holocene* **7**, 361–370 (1997).
37. J. González, J. B. Valdés, Bivariate drought recurrence analysis using tree-ring reconstructions. *J. Hydrol. Eng.* **8**, 247–258 (2003).
38. J. T. Shiau, Fitting drought duration and severity with two-dimensional copulas. *Water Resour. Manag.* **20**, 795–815 (2006).
39. I. Kojadinovic, J. Yan, Modeling multivariate distributions with continuous margins using the copula R package. *J. Stat. Softw.* **34**, 1–20 (2010).
40. J. Esper, D. C. Frank, R. J. S. Wilson, K. R. Briffa, Effect of scaling and regression on reconstructed temperature amplitude for the past millennium. *Geophys. Res. Lett.* **32**, L07711 (2005).
41. A. W. Bowman, A. Azzalini, *Applied Smoothing Techniques for Data Analysis: The Kernel Approach with S-Plus Illustrations* (OUP Oxford, 1997).
42. J. Hansen, R. Ruedy, M. Sato, K. Lo, Global surface temperature change. *Rev. Geophys.* **48**, RG4004 (2010).
43. C.-Y. Xu, V. P. Singh, Cross comparison of empirical equations for calculating potential evapotranspiration with data from Switzerland. *Water Resour. Manag.* **16**, 197–219 (2002).
44. G. P. Compo, J. S. Whitaker, P. D. Sardeshmukh, N. Matsui, R. J. Allan, X. Yin, B. E. Gleason, R. S. Vose, G. Rutledge, P. Bessemoulin, S. Brönnimann, M. Brunet, R. I. Crouthamel, A. N. Grant, P. Y. Groisman, P. D. Jones, M. C. Kruk, A. C. Kruger, G. J. Marshall, M. Maugeri, H. Y. Mok, Ø. Nordli, T. F. Ross, R. M. Trigo, X. L. Wang, S. D. Woodruff, S. J. Worley, The twentieth century reanalysis project. *Q. J. Roy. Meteorol. Soc.* **137**, 1–28 (2011).
45. I. Harris, P. D. Jones, T. J. Osborn, D. H. Lister, Updated high-resolution grids of monthly climatic observations – The CRU TS3.10 Dataset. *Int. J. Climatol.* **34**, 623–642 (2014).

Acknowledgments: We are grateful for the support of field and laboratory technicians K. Allen, D. Martin-Benito, J. Burkhart, S. Cockrell, K. de Graauw, J. James, J. Martin-Fernandez, G. Munkhbat, S. Nichols, E. Orsoo, B. Soronzonbold, B. Ulziibayar, and J. Zhu. **Funding:** This research was made possible through grants from the National Geographic (9114-12), the NSF (CNH-1210360 and DEB-0816700), the West Virginia University Faculty Senate, and The Climate Center of Lamont-Doherty Earth Observatory. Lamont-Doherty Earth Observatory contribution 8194. B.C. was supported by the NASA Modeling, Analysis, and Prediction program. **Author contributions:** A.E.H. and K.J.A. conceptualized the paper. A.E.H. and N.P. made the tree ring collections with C.L., O.B., K.J.A., and B.N. A.E.H., L.A.H., and C.L. standardized the tree ring measurements and developed the reconstruction. A.E.H., K.J.A., C.J., and B.C. analyzed the proxy and climate model data. A.E.H., K.J.A., and C.J., prepared figures. A.E.H. and K.J.A. led the study, and the remaining authors assisted with data interpretation and manuscript preparation. H.T. provided feedback on the concept, data interpretation, and manuscript preparation. **Competing interests:** The authors declare that they have no competing interests. **Data and materials availability:** Upon publication, tree ring data will be deposited in the International Tree Ring Databank (https://www.ncdc.noaa.gov/data-access/paleoclimatology-data). The CMIP5 multimodel ensemble data can be obtained from the Lawrence Livermore National Laboratory (https://esgf-node.llnl.gov/projects/esgf-llnl/). CSM LME data can be obtained from the Community Earth System Model: Last Millennium Ensemble Project (www.cesm.ucar.edu/projects/community-projects/LME/). All other data needed to evaluate the conclusions in the paper are present in the paper and/or the Supplementary Materials. Additional data related to this paper may be requested from the authors.

Submitted 31 May 2017
Accepted 7 February 2018
Published 14 March 2018
10.1126/sciadv.1701832

Citation: A. E. Hessl, K. J. Anchukaitis, C. Jelsema, B. Cook, O. Byambasuren, C. Leland, B. Nachin, N. Pederson, H. Tian, L. A. Hayles, Past and future drought in Mongolia. *Sci. Adv.* **4**, e1701832 (2018).

Past and future drought in Mongolia

Amy E. Hessl, Kevin J. Anchukaitis, Casey Jelsema, Benjamin Cook, Oyunsanaa Byambasuren, Caroline Leland, Baatarbileg Nachin, Neil Pederson, Hanqin Tian and Laia Andreu Hayles

Sci Adv **4** (3), e1701832.
DOI: 10.1126/sciadv.1701832